Pharmaceutical Research, Vol. 26, No. 4, April 2009 (© 2008)
DOI: 10.1007/s11095-008-9779-9

Research Paper

Lactose Composite Carriers for Respiratory Delivery

Paul M. Young,[1,2] Philip Kwok,[1] Handoko Adi,[1] Hak-Kim Chan,[1] and Daniela Traini[1]

Received June 25, 2008; accepted October 30, 2008; published online November 18, 2008

Purpose. Lactose dry powder inhaler (DPI) carriers, constructed of smaller sub units (composite carriers), were evaluated to assess their potential for minimising drug–carrier adhesion, variability in drug–carrier forces and influence on drug aerosol performance from carrier–drug blends.
Methods. Lactose carrier particles were prepared by fusing sub units of lactose (either 2, 6 or 10 μm) in saturated lactose slurry. The resultant composite particles, as well as supplied lactose, were sieve fractioned to obtain a 63–90 μm carriers. The carriers were evaluated in terms of size (laser diffraction) morphology (electron microscopy and atomic force microscopy), crystallinity and drug adhesion (colloid probe microscopy). In addition, blends containing drug and carrier were prepared and evaluated in terms of drug aerosol performance.
Results. The surface morphology and physico-chemical properties of the composite carriers were significantly different. Depending on the initial primary lactose size, the composite particles could be prepared with different surface roughness. Variation in composite roughness could be related to the change in drug adhesion (via modification in contact geometry) and thus drug aerosol performance from drug–lactose blends.
Conclusion. Composite based carriers are a potential route to control drug–carrier adhesion forces and variability thus allowing more precise control of formulation performance.

KEY WORDS: colloid probe microscopy; DPI composite; dry powder inhalation; inhalation.

INTRODUCTION

The delivery of dry powder particulates to the lung for respiratory therapy requires the active pharmaceutical ingredient (API) to have an aerodynamic diameter <6 μm (1). Furthermore, the dose of API (often ≤400 μg dose^{-1}) requires dilution with excipient material to increase dose reproducibility and improve flow during manufacturing and handling. The most common formulation approach is to blend the API with a larger 'inert' excipient (referred to as a carrier); such as lactose.

The dynamic blending process between two materials (containing size differentials of an order of magnitude as seen in DPI formulations) results in an ordered mix (2). Although the distribution of API throughout such ordered mixes tend to be uniform (observed via content uniformity measurement) variations in the properties of the API, carrier and environment may cause large variations in inter-particle forces. Clearly, any change in the force of API–carrier interaction will have a direct affect on the aerosolisation efficiency of the API when inhaled, since the force required to separate the drug from carrier will be altered.

Inter-particle adhesion in carrier-based DPI systems may be attributed to multiple factors including surface energy (3), relative humidity (4–7), morphology of the API (8–10), the presence of ternary components (11–13) and morphology of the carrier (14–16). To complicate matters, the lack of homogeneity across the surface of a carrier results in a distribution of adhesion forces which may be classified as iso-energetic regions or 'active sites' (2,17). The distribution of a range of adhesion forces across the surface of a carrier may promote variability in drug detachment with the higher energy sites terminating drug liberation (18).

To overcome high drug–carrier adhesion and/or variability, the carrier may be modified using processes such as coating (15,19–21), etching (15,22) or the addition of fine material (11,12,23). However, these processes either introduce ternary components that require regulatory scrutiny or reduce variability in adhesion with little control over the median adhesion value (i.e. surface variability is reduced but adhesion is limited to the contact geometry of the planar surface of each crystal face).

To overcome the limitations of conventional carrier surfaces, we have investigated the potential use of composite carriers for controlling adhesion variability and drug–carrier contact geometry (24). By constructing a course carrier from smaller sub units, of similar or smaller size than the API, the contact geometry may be varied and thus adhesion controlled. Furthermore, since the carrier is constructed from many smaller units, a homogeneous surface roughness may be produced. In the previous study, the group used a sugar

[1] Advanced Drug Delivery Group, Faculty of Pharmacy, University of Sydney, Sydney, NSW 2006, Australia.
[2] To whom correspondence should be addressed. (e-mail: py@pharm.usyd.edu.au)

alcohol, mannitol, as the excipient of choice (due to its highly crystalline nature) (24). To expand on this study, the authors investigate commonly used DPI excipient; lactose.

A series of lactose composite particles were engineered and evaluated in terms of morphology, size, drug–carrier adhesion and aerosolisation performance from conventional DPI systems.

MATERIALS AND METHODS

Materials

Lactose monohydrate (Lactochem® crystals) was supplied by Friesland Foods Domo (Zwolle, The Netherlands). The model drug, micronised salbutamol sulphate was supplied by 3M (St. Paul, MN, USA). Water was purified by reverse osmosis (Milli-Q, Sydney, Australia). All solvents used throughout were supplied by Biolab (Clayton, VIC, Australia) and were of analytical grade.

Preparation of Carrier Particles

A series of primary micron-sized lactose particles were prepared by spray drying an aqueous solution of lactose using a Mini Spray Dryer (Büchi, B-290, Switzerland). Spray drying conditions for each target particle diameter are shown in Table I. The prepared powders were stored in a tightly sealed container with silica gel for a minimum of 24 h prior to composite formation. After storage, the primary lactose particles were mixed with a 10% *v/w* saturated lactose aqueous slurry and passed through a 180 μm sieve. The resultant aggregates were dried at 150°C for 1.5 h in a mini fluid bed dryer (Umang Pharmatech Ltd. Easton, PA, USA). The composite powders were collected and stored for 24 h as before, prior to sieving. The subsequent fused aggregates were processed through a nest of sieves to produce a 63–90 μm sieve fraction. In addition, the starting α-lactose monohydrate raw material was processed through the same nest of sieves to obtain a similar size fraction for comparison. Four carrier powders were produced; composites based on 2, 6 and 10 μm primary particles (referred to as 2, 6 and 10 μm carriers for ease of reference) as well as the regular carrier (sieved directly from the starting material).

Scanning Electron Microscopy

The morphology of the carrier particles was investigated using scanning electron microscopy (SEM). Samples were deposited on carbon sticky tabs, mounted on a SEM stubs and sputter coated with 15–20 nm gold prior to imaging. The carrier particles were imaged at 10 keV using a field emission SEM (FESEM JEOL 6000, JEOL, Japan).

Atomic Force Microscopy

The topography of each carrier was studied with conventional Tapping Mode® atomic force microscopy (AFM) (Multimode AFM, Nanoscope IIIa controller, Veeco Inc., California, USA). Samples were mounted on carbon sticky tabs and imaged with a high aspect ratio silicon probe (MicroMasch tips, Group Scientific Ltd, Adelaide, Australia) at a scan rate of 1.0 Hz. Three 10×10 μm areas were studied for each carrier.

Particle Size Analysis

The particle size distributions of the micronised salbutamol sulphate, primary lactose particles and carriers were investigated using laser diffraction. Samples were analysed using the Malvern Mastersizer 2000 with Scirocco dry powder feeder (Malvern, UK). The micron-sized powders were analysed using a 400 kPa pressure differential while the carrier systems were analysed at 100 kPa. Samples were analysed in triplicate at an obscuration between 0.3% and 10.0%. Refractive indices of 1.540 and 1.553 were used for lactose and salbutamol sulphate samples, respectively.

X-ray Powder Diffractometry

The crystalline properties of the primary lactose particles and four carriers were investigated using X-ray powder diffraction. Samples were analysed at room temperature with a XRPD D5000 (Siemens, Munich, Germany) using CuKα radiation at 30 mA and 40 kV. An angular increment of $0.05°s^{-1}$ and count time of 2 s was used.

Differential Scanning Calorimetry

The thermal response of the primary lactose particles and carrier systems were evaluated using differential scanning calorimetry (DSC). Approximately 10 mg of the sample was accurately weighed into DSC sample pans and crimp-sealed. Samples were analysed using a DSC 823E (Mettler Toledo, Melbourne, Australia). Thermal properties analysed at between 10°C and 250°C a $10°C\ min^{-1}$ temperature ramp.

Colloidal Probe Microscopy

Colloid probe microscopy was used to measure the force of adhesion between individual salbutamol sulphate particles and each carrier. Individual particles of micronised salbutamol sulphate were mounted onto the apex of 0.58 N m^{-1} spring constant tipless AFM cantilevers (NP-OW, Veeco, Cambridge UK), using methods and validation described elsewhere (25–27). Prior to measurement, particles of each carrier were mounted

Table I. Spray Drying Conditions for the Preparation of Primary Lactose Particulates

Target particle size (μm)	Inlet temperature (°C)	Outlet temperature (°C)	Aspiration (%)	Atomising air flow (Normlitre h^{-1})	Liquid feed rate (mL min^{-1})	Aqueous lactose solution (g L^{-1})
2	150	80	100	819	5	150
6	150	89	100	357	5	150
10	150	97	100	246	5	200

on carbon sticky tabs and attached to AFM sample stubs. The force of cohesion between each drug probe and both regular and composite carrier was investigated in Force Volume mode, where 4,096 individual force curves were conducted over 10×10 μm. The following settings were utilised: approach-retraction cycle, 2 μm; cycle rate, 8.33 Hz; and constant compliance region 60 nm. Each curve in the force volume matrix was analysed using custom-built software and exported as 4,096 force of cohesion values for data analysis. Three salbutamol sulphate tips were studied on each carrier at 45% RH and 25°C.

Preparation and Characterisation of Drug–Carrier Blends

Each 63–90 μm sieve fractioned carrier was blended with salbutamol sulphate based on methods described elsewhere (5). Briefly, salbutamol sulphate was blended geometrically with carrier at a ratio of 1:67.5, prior to a final mix in a Turbula (Willy A. Bachofen AG Maschinenfabrik, Basel, Switzerland) at 46 rev^{-1} for 30 min. After blending samples were stored in tightly sealed containers at 45% RH and 25°C, for a minimum of 24 h prior to analysis.

High performance liquid chromatography (HPLC) was utilised to analyse salbutamol sulphate from the *in vitro* aerosol performance studies and content uniformity measurements. The HPLC used was a Waters™ Millennium system (Waters Ltd., Sydney, Australia) using system components and conditions reported previously (5).

The mobile phase used consisted of a 60:40 v/v methanol: water mixture containing 0.1% *w/v* sodium lauryl sulphate. Samples were dissolved in MilliQ water. Linearity was obtained between 0.5 and 100 μg mL^{-1} (R^2=0.9990) with a retention time of approximately 5 min. Collected samples were appropriately diluted to fit within this region.

Prior to *in vitro* aerosol evaluation of the blends, each formulation was tested for content uniformity. Approximately 33 mg of each blend was diluted with MillQ water and analysed using the HPLC method described previously. Analysis of the content uniformity data suggested all formulations to have a coefficient of variance <5% (n=5).

The aerosol performance of micronised salbutamol sulphate from each drug–carrier formulation was investigated using the next generation impactor (NGI). The NGI (Apparatus E, British Pharmacopeia, Appendix XXI F) is an eight-stage inertial impactor that separates an aerosol cloud into discrete size ranges based on aerodynamic diameter. The method followed that specified for DPIs in the pharmacopoeia (Appendix XXI F). All *in vitro* measurements were conducted at 60 L min^{-1}, (obtained using a Rotary vein pump and solenoid valve timer, Erweka GmbH, Germany) which was set using a calibrated flow meter (TSI 3063, TSI instruments Ltd., Buckinghamshire, UK). Prior to testing, all eight-collection stages were coated with silicon oil to eliminate particle bounce and the NGI pre-separator was accurately filled with 15 mL of MillQ water.

A Cyclohaler™ (Novartis, Surrey, UK) was used as a model DPI device. Approximately 33 mg of formulation was accurately weighed into a size-3 gelatine capsule (Capsugel, Sydney, Australia), which was placed into the sample compartment of a DPI. The device was activated, connected to a mouthpiece adapter, inserted into a United State Pharmacopoeia (USP) throat (connected to the NGI) and tested for 4 s at 60 L min^{-1}. After actuation, the device, capsule, mouthpiece adapter, throat, pre-separator and all sample stages were washed into separate volumetrics using water. Each blend was tested in triplicate.

Statistical Analysis

Data were subjected to analysis of variance (ANOVA) (Minitab 12.1, Minitab Ltd., Coventry, UK). Significant differences between formulations were analysed using post hoc multiple comparisons and p values of <0.05 (Fisher Pair wise) were considered to be significant.

RESULTS AND DISCUSSION

Particle Size Analysis

Size distributions of the primary particles and salbutamol sulphate are shown in Fig. 1A, while the engineered carriers are shown in Fig. 1B. The salbutamol sulphate particle size distribution had a median diameter ($d_{0.5}$) of 1.39±0.05 μm with 90% of particles ($d_{0.9}$) less than 2.71±0.14 μm, suggesting the micronised drug to be of a suitable size for inhalation. The spray dried primary lactose particles, used to engineer the composite carriers had $d_{0.5}$ diameters of 2.27±0.12, 6.15±

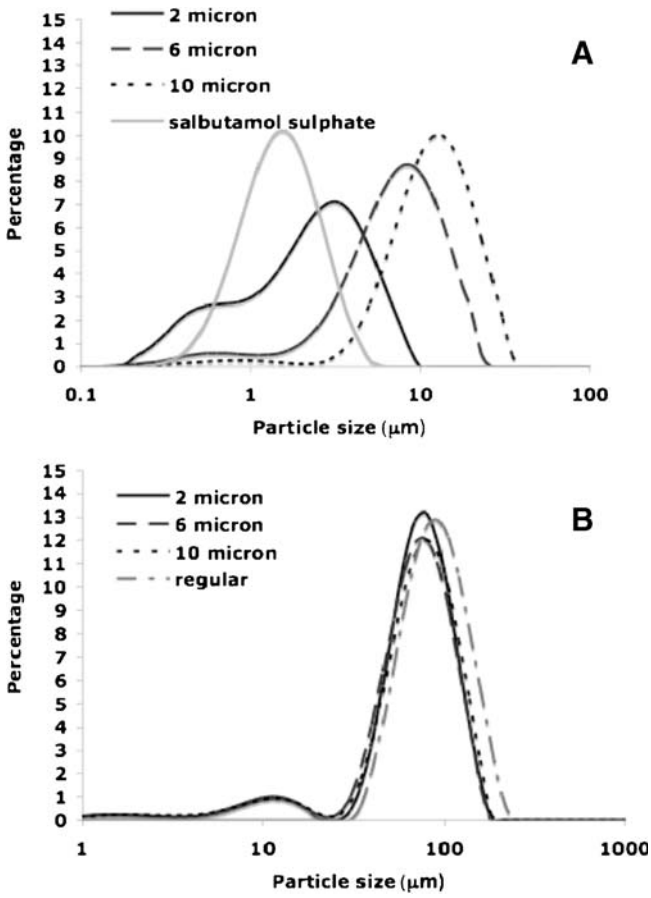

Fig. 1. Particle size distributions of the **A** micronised drug samples and primary lactose particles, **B** carrier particles.

0.50 and 10.75±0.09 μm. These particle size distributions were labelled as 2, 6 and 10 μm, for easy reference. Analysis of the sieve fractioned carriers (Fig. 1B) suggested similar $d_{0.5}$ values of 77.72, 74.67, 78.82 and 94.88 μm for the 2, 6, 10 μm based composite and regular carriers, respectively. Such observations are expected, since the four carriers were fractioned through a 63–90 μm sieve.

Scanning Electron Microscopy

Representative scanning electron micrographs of the sieve fractioned composite and regular carrier particles are shown in Fig. 2. All carriers appeared to have similar macroscopic morphology and size distributions. This is expected since all carriers were processed through a 63–90 μm sieve. Higher resolution images showed distinct variations between the regular carrier (Fig. 2A) and the composite carriers (Fig. 2B,C). In general, the regular carrier particles were formed as discrete singular crystals of the sieve fractioned range whereas the composite carriers were macroscopically similar in dimension to the regular carrier, but were composed of multiple micron-sized particles appearing crystalline in nature. In addition, qualitative analysis of the composite carriers suggested an increase the in the primary micro-particle size between the 2 and 10 μm based composite carriers, respectively. However, it is interesting to note, that the individual particles making up the composite (particularly, for example, in the larger 10 μm-based carriers) did not have a similar diameter to the median $d_{0.5}$ of the primary particles, measured by laser diffraction. Such observations can be explained by the re-crystallisation of the primary particles during the drying process. To further quantify the variations in surface morphology, atomic force microscopy was utilised to study the surface topography of each carrier.

Atomic Force Microscopy

Representative topographical images of the composite and regular carriers are shown in Fig. 3A–D. Clear variations in the topography could be observed across the carrier types. Specifically, the regular carrier (Fig. 3A) had a smooth planar morphology while the composite materials were granular in nature; most likely due to the individual microparticles, which make up their construction. To further evaluate these variations the root mean square roughness (R_{RMS}) for each image was calculated using Eq. 1:

$$R_{RMS} = \sqrt{\frac{1}{n}\sum_{i=1}^{n} y_i^2} \quad (1)$$

where n is the number of points in topography profile and y_i is the distance of a point i from the centre line.

Analysis of the R_{RMS} suggested the carriers (n=3 for each carrier) followed the rank order 2 μm>6 μm>10 μm composite carriers>regular carrier. Specifically, analysis of the

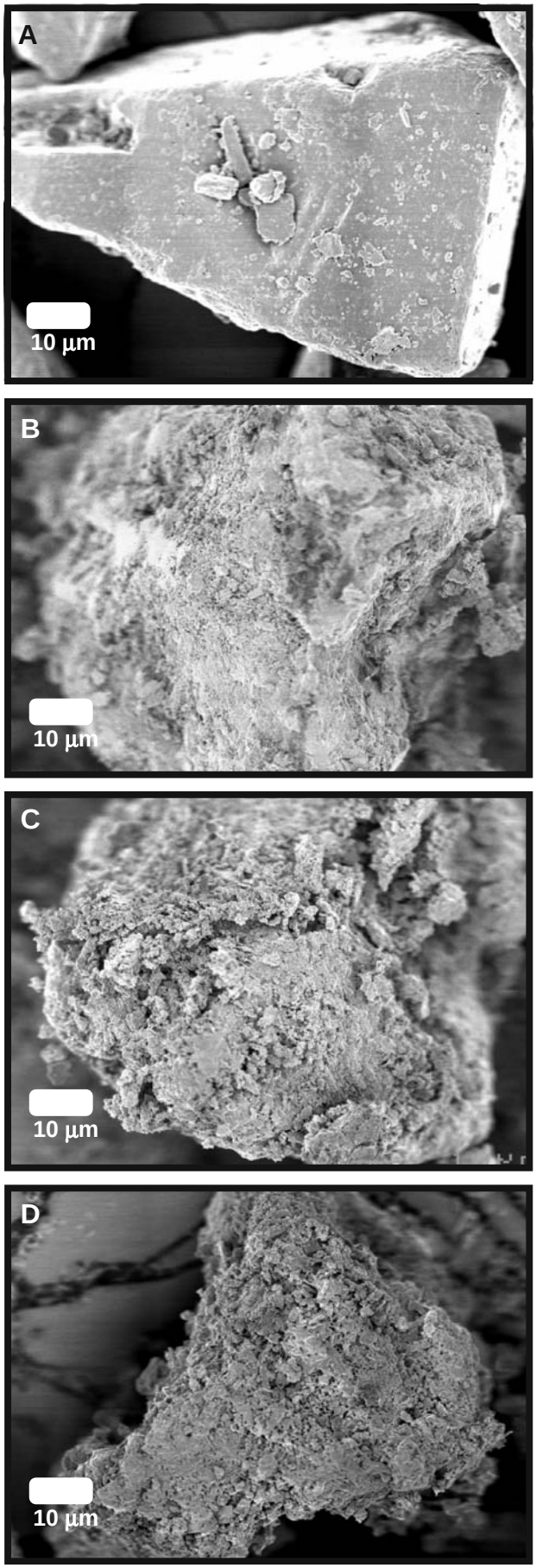

Fig. 2. Scanning electron microscopy images of fractioned **A** regular carrier, **B** 2 μm based carrier, **C** 6 μm based carrier and **D** 10 μm based carrier.

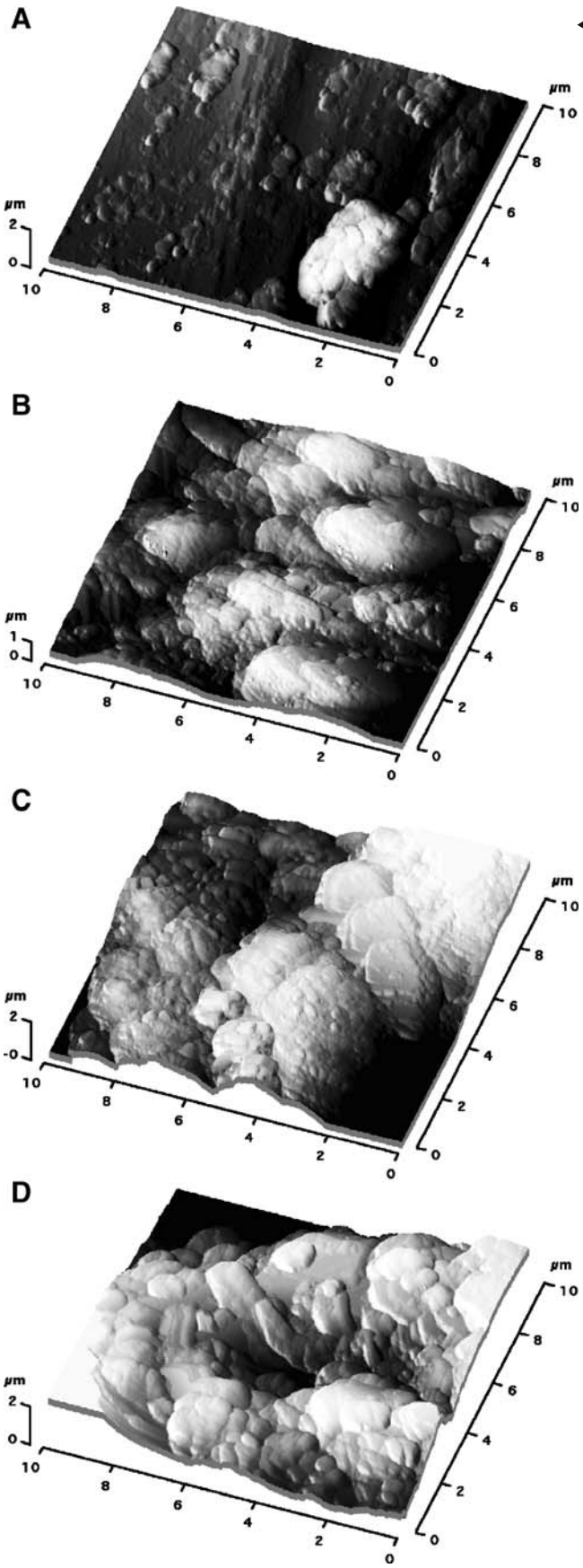

Fig. 3. Representative topographical images of the 63–90 μm sieve fractioned **A** regular carrier, **B** 2 μm composite carrier, **C** 6 μm composite carrier and **D** 10 μm composite carrier.

R_{RMS} indicated significantly different values of 0.50±0.01, 0.36±0.01, 0.32±0.01 and 0.09±0.05 μm for 2, 6, 10 μm composite carriers and regular carrier, respectively. Such observations suggest that variation in primary particle size has a significant effect on the composite particle roughness.

X-ray Powder Diffractometry

X-ray powder diffractograms of the primary lactose particles and carriers are shown in Fig. 4A and B, respectively. The diffuse diffraction patterns for the primary lactose particles (Fig. 4A) are indicative of an amorphous material. In comparison, the diffraction patterns for the carrier materials had intensity patterns characteristic of crystalline material. In general, the diffraction patterns for the carrier materials (Fig. 4B) were similar and had peaks characteristic of α-lactose monohydrate at 12.4° 2θ (28). The composite carrier diffraction patterns had intensities less than that of the regular carrier,

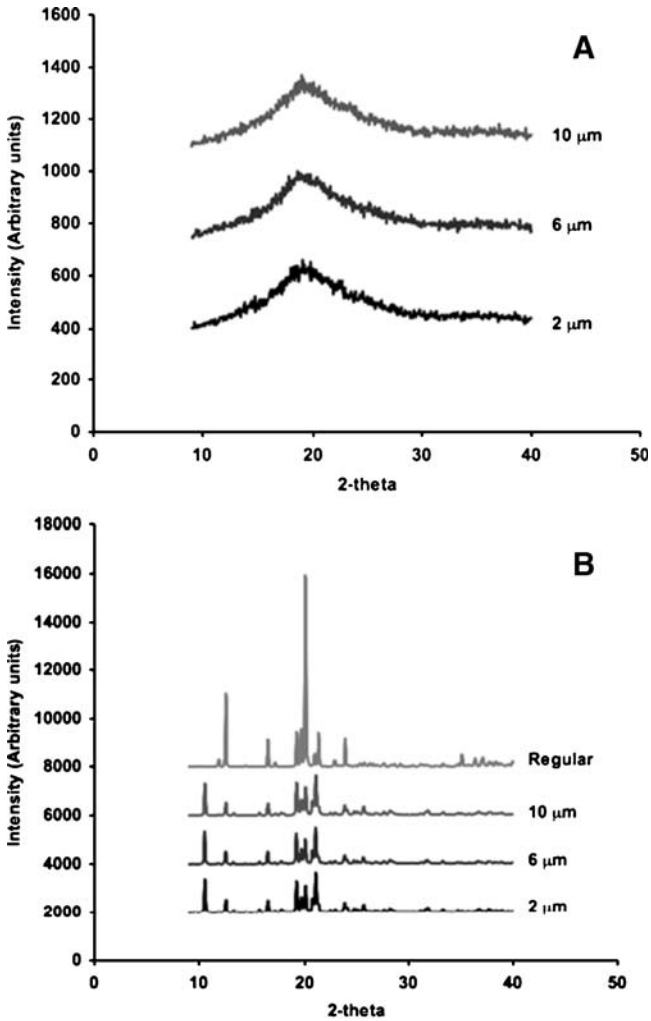

Fig. 4. X-ray powder diffractograms for the **A** primary lactose particles and **B** composite carriers.

most likely due to the significant difference in the primary crystal size (2–10 μm in comparison to 63–90 μm). Interestingly, the composite carriers had an additional peak at 10.6° 2θ, suggesting the presence of β-lactose (28) which is produced due to the mutarotation of the α-form during the drying process (29).

Differential Scanning Calorimetry

Differential scanning thermograms for the four primary lactose particles and four carriers are shown in Fig. 5A and B, respectively. As expected, the thermal response for the primary particles was indicative of an amorphous material. Specifically, an exothermic peak for each powder was observed with an onset between 130°C and 140°C. This is similar to previous reports (30) for re-crystallisation of amorphous lactose. Interestingly, the onset increased with increasing median particle diameter. It is suggested that this increase is due to an increase in heat capacity and reduction in surface area to mass ratio. In comparison, the thermal response of the carrier materials (Fig. 5B) was characteristic of crystalline material. For all samples, an endothermic peak was observed between 140°C and 150°C, which could be attributed to the heat of dehydration (30,31) from α-lactose monohydrate. In addition, comparison of the regular and composite carrier suggested different endothermic peaks at 216°C for the regular and peaks at 216°C and 235°C for the composite carriers. These peaks at 216°C and 235°C correspond to the α-lactose monohydrate and β-lactose, respectively (31). Such observations suggest that the composite carriers were a mixture of both α-lactose monohydrate and β-lactose, most likely due to the mutarotation of the α-form during the final drying stage (post slurry) (28).

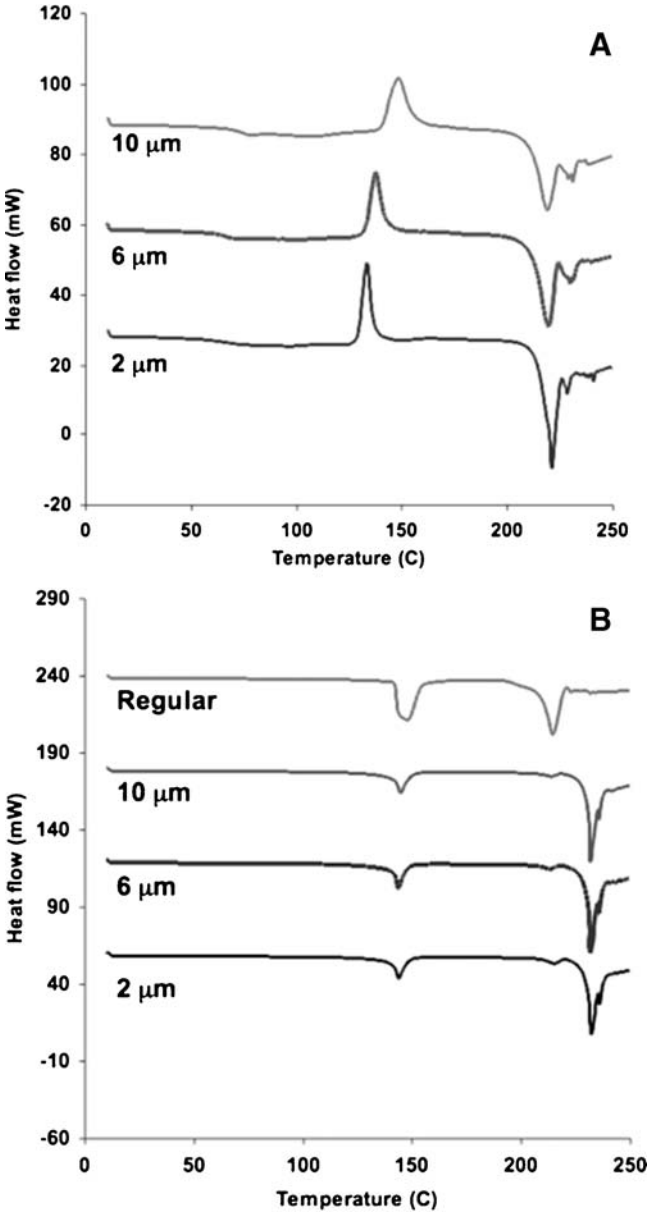

Fig. 5. Differential scanning calorimetry thermograms of **A** primary lactose particles and **B** composite carriers.

Colloidal Probe Microscopy

Adhesion data collected between each salbutamol sulphate drug probe (n=3 probes×4,096 force measurements over 10×10 μm areas) were processed to produce median force values ($f_{0.5}$) and percentile under-force values. The processing methodology followed that for log-normal force distributions as described previously (24). In addition the spread of force values was calculated from the geometric standard deviation (GSD) (32):

$$GSD = \left[\frac{f_{0.84}}{f_{0.16}}\right]^{0.5} \quad (2)$$

where f_x are the respective percentile force values for the lognormal distribution (32).

Analysis of the adhesion data suggested significant differences in adhesion force between the salbutamol sulphate drug probes (n=3) and the different carriers. In general, the median adhesion force followed the rank order: 2 μm composite carrier<6 μm composite carrier<10 μm composite carrier<regular carrier. Specifically, median adhesion forces (±standard deviations) of 30.15±0.75, 33.31±6.32, 46.43±3.83 and 113.11±15.10 nN were observed for the 2, 6, 10 μm composite carriers and regular carrier, respectively. Post-hoc analysis suggested the variation in adhesion to be significant between all paired and unpaired samples except for the 2 and 6 μm paired analysis. Such observations are most likely due to the large standard deviation in adhesion forces on the 6 μm based carrier. Since variation in adhesion across the surface may be directly related to the propensity for drug liberation during aerosolisation, the GSD for each data set was calculated and processed to represent mean GSD values (±standard deviations) and are shown along representative adhesion maps in Fig. 6. The degree of colour variation in Fig. 6 indicates the distribution in force values. Analysis of the mean GSD, suggested a rank order of 2 μm<10 μm< 6 μm<regular based carrier systems. Furthermore, analysis of the GSD between samples (n=3 carrier measurements) resulted in a greater variation in the 6 μm and regular carriers, where a coefficient of variation (CV) of 15.1% and 10.5% was

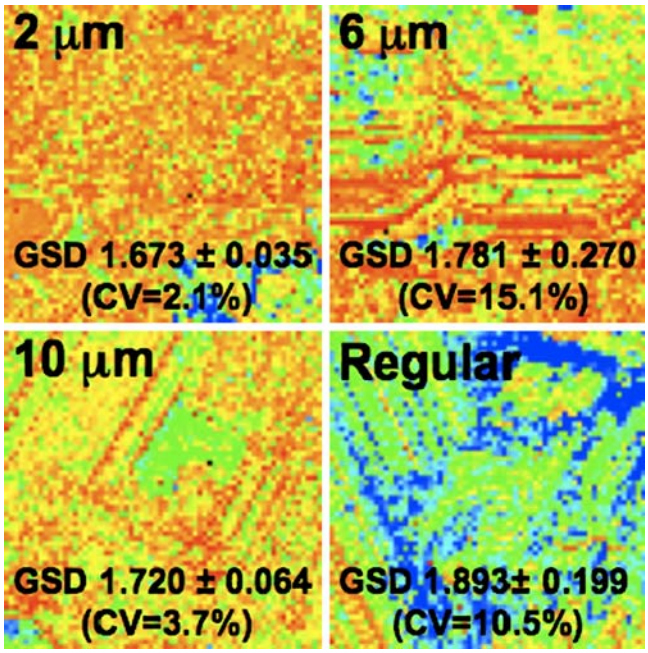

Fig. 6. Adhesion distribution matrix (10×10 μm areas) for a single salbutamol sulphate probe on each composite carrier lactose. Mean GSD values are given for $n=3$ probes with standard deviations and percent CV.

observed, respectively. In comparison, the 2 and 10 μm carriers exhibited reduced adhesion value distributions.

In vitro Aerosol Characterisation

The drug recovered from all components of the NGI and device was measured by HPLC as previously described and the data was processed to produce various descriptors of aerosolisation efficiency. These were the total recovered dose from the device and all NGI components (TD); the emitted dose (ED), representing TD excluding capsule and device components; the fine particle dose (FPD) representing drug recovered from stage 3 to 8 of the NGI (equivalent to the mass of particles with an aerodynamic diameter <4.46 μm). In addition, the percentage drug deposited on each stage was calculated for each formulation and is plotted in Fig. 7. Analysis of the TD and ED suggested no significant differences with recoveries of 514.9±44.8 and 431.7±32.5 μg being observed across all formulations. Subsequently, no variations in drug removal efficiency were observed (ED/TD×100). An efficiency of 84±6% across all formulations was in good agreement with previous findings (5). Since the efficiency remained constant it may be assumed that the variation in FPD may be due to drug carrier detachment during aerosolisation and not due to formulation segregation prior to analysis. This is further substantiated by the content uniformity results, which showed all formulations to have a variability (CV) less than 5%.

Analysis of the percentage stage deposition (Fig. 7) showed the regular carrier had less drug deposited on the lower stages with the majority being captured on the pre-separator. High depositions on the pre-separator stage may be associated with drug still adhered to carrier after the aerosolisation process. In comparison, the deposition profiles of drug from the composite carrier systems indicated higher depositions in the lower stages of the NGI suggesting improved aerosol performance. To further analyse the relationship between carrier type and aerosolisation efficiency, the fine particle fraction was calculated based on the ED (where FPF=FPD/ED×100). Analysis of the FPF data suggested the carrier type to have a significant effect on the

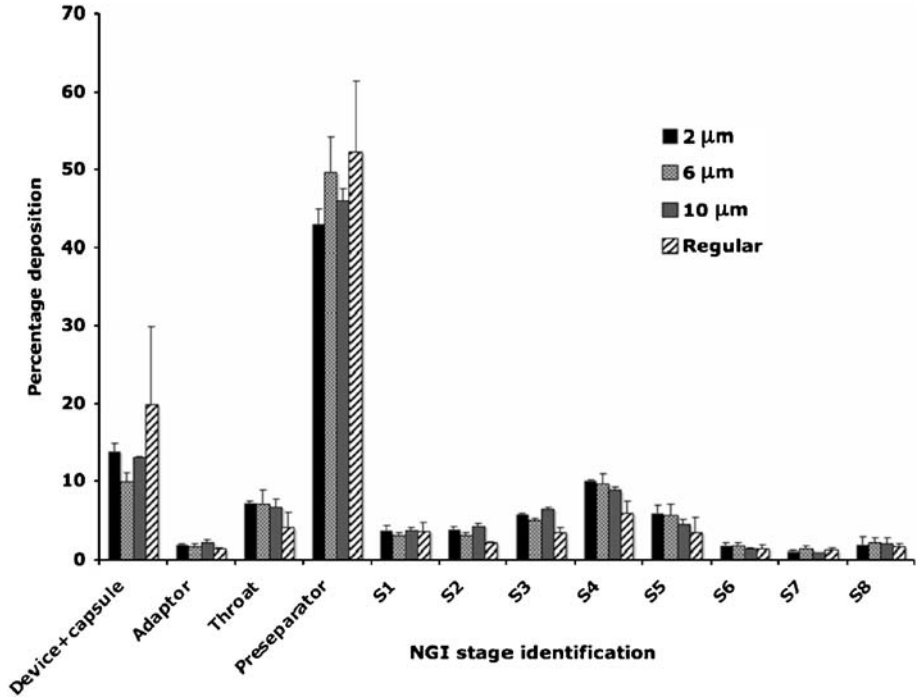

Fig. 7. *In vitro* NGI stage deposition of salbutamol sulphate aerosolised from each of the composite carriers.

aerosolisation performance where the FPF varied between 21.3±5.4% and 31.3±1.3% between regular lactose and the 2 μm composite lactose, respectively. In addition, analysis of the standard deviations of the FPFs from each formulation suggested CV to be dependent upon formulation type where FPF CV's of 4%, 13%, 5% and 25% were observed for the 2 μm, 6 μm, 10 μm and regular carrier, respectively.

Relationship between Drug Aerosol Performance and the Physico-chemical Parameters of the Carrier Systems

To further understand the relationship between the different carrier systems and drug aerosol performance, the FPF was investigated in terms of each of the physico-chemical parameters studied. One of the primary differences between the regular and composite carriers was the presence of β-lactose in the composite samples. Interestingly, there was still variation in the FPF in the composite samples although the heat of dehydration remained constant. Such observations indicate that particle morphology plays an important role in the aerosolisation phenomena. Furthermore, previous studies have suggested that β-lactose results in significantly poorer aerosolisation performance than α-lactose monohydrate (33). In this previous study, formulations containing micronised salbutamol sulphate were used with identical formulation and testing protocols (33). Subsequently, it may be concluded that in this study, while there was variation in carrier chemistry, the variation between the regular and composite carriers is more dependent on morphology.

Evaluation of the topographic roughness suggested significant differences between the carrier particles. To investigate the relationship between roughness and aerosolisation performance, the FPF was plotted as a function of R_{RMS} and is shown in Fig. 8. Regression analysis of the FPF *vs*. R_{RMS} indicated a positive linear relationship with an R^2 value of 0.9672. Such an increase in FPF with respect to roughness may be related to the reduced contact area between drug particles and carrier surface (10,14,24).

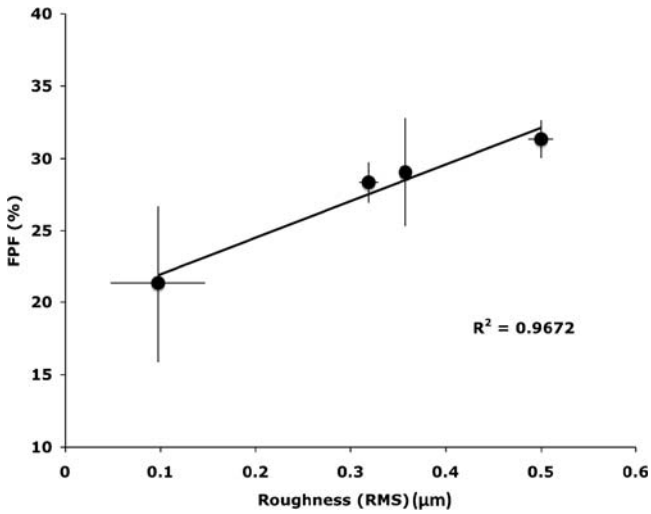

Fig. 8. *In vitro* aerosol performance (FPF) of the composite carriers as a function of roughness (R_{RMS}). Error bars indicate standard deviations (n=3).

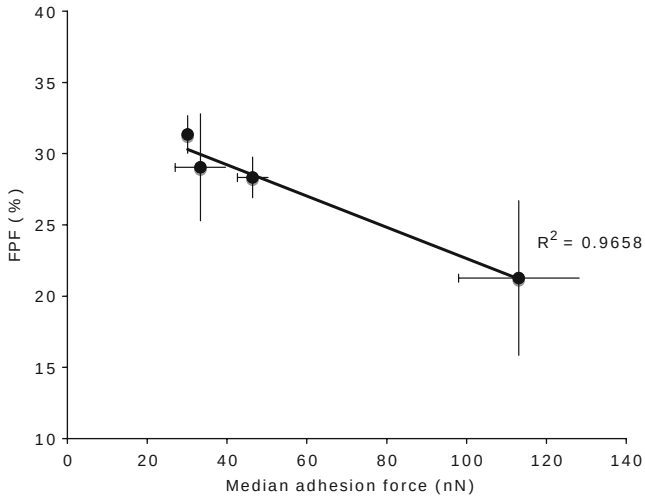

Fig. 9. Relationship between median adhesion force (n=3 tips±SD) and the aerosol efficiency (FPF%, n=3) of the composite carriers.

As previously discussed, a reduction in drug–carrier contact area would result in reduced inter-particle adhesion. To investigate the relationship between aerosolisation efficiency and drug–carrier adhesion, the FPF was plotted *vs*. the median adhesion force values and are shown in Fig. 9. An inverse relationship between FPF and the median adhesion force was observed, with a regression coefficient of R^2= 0.9658 (similar to that for the FPF-roughness analysis). It may be concluded that a clear relationship exists between contact area (in this case measured by a R_{RMS} roughness parameter), drug–carrier adhesion and aerosol performance. In addition, it is interesting to note, the relationship between the standard deviation of the FPF measurements and the geometric standard deviation of the adhesion measurements. For example, a large standard deviation is associated with the FPF of drug from the 6 μm composite carrier even though content uniformity was <5% and the aerosolisation efficiency was not significantly different than the other carrier systems. Subsequently, it may be concluded that the variation in FPF is due to a wider distribution in the adhesion force between drug and carrier on the surface. Indeed, analysis of the median adhesion forces for drug on the 6 μm composite carriers had a greater standard deviation than for the other composite systems (Fig. 9). Such observations are further corroborated when studying the GSD values for the adhesion measurement (indicative of data spread) and the CV associated with multiple area analysis (Fig. 6). As expected, larger variations in adhesion and FPF were found in the regular carrier, which could be associated to the poorer FPF and standard deviation.

CONCLUSIONS

A series of crystalline composite carriers were prepared from smaller sub-units of lactose. The surface morphology and physico-chemical properties of the composite carriers were significantly different than regular α-lactose monohydrate. Depending on the initial primary lactose size, the composite particles could be prepared with different surface

roughness. Variation in composite roughness could be related to the change in drug adhesion (via modification in contact geometry) and thus drug aerosol performance from drug–lactose blends. Although, in all cases the composite carriers resulted in improved drug aerosol performance, it should be noted that the distribution of adhesion potential across each carrier was specific to the primary size. Thus it may be concluded that, careful selection of surface roughness is required to optimise aerosol performance and reduce the variability in respiratory delivery.

REFERENCES

1. J. N. Pritchard. The influence of lung deposition on clinical response. *J. Aerosol Med*. **14**:S19–S26 (2001). doi:10.1089/08942680150506303.
2. J. A. Hersey. Ordered mixing—new concept in powder mixing practice. *Powder Technol*. **11**:41–44 (1975). doi:10.1016/0032-5910(75)80021-0.
3. D. Cline, and R. Dalby. Predicting the quality of powders for inhalation from surface energy and area. *Pharm. Res*. **19**:1274–1277 (2002). doi:10.1023/A:1020338405947.
4. R. Price, P. M. Young, S. Edge, and J. N. Staniforth. The influence of relative humidity on particulate interactions in carrier-based dry powder inhaler formulations. *Int. J. Pharm*. **246**:47–59 (2002). doi:10.1016/S0378-5173(02)00359-9.
5. P. M. Young, A. Sung, D. Traini, P. Kwok, H. Chiou, and H. K. Chan. Influence of humidity on the electrostatic charge and aerosol performance of dry powder inhaler carrier based systems. *Pharm. Res*. **24**:963–970 (2007). doi:10.1007/s11095-006-9218-8.
6. V. Berard, E. Lesniewska, C. Andres, D. Pertuy, C. Laroche, and Y. Pourcelot. Dry powder inhaler: influence of humidity on topology and adhesion studied by AFM. *Int. J. Pharm*. **232**:213–224 (2002). doi:10.1016/S0378-5173(01)00913-9.
7. X. M. Zeng, H. B. MacRitchie, C. Marriott, and G. P. Martin. Humidity-induced changes of the aerodynamic properties of dry powder aerosol formulations containing different carriers. *Int. J. Pharm*. **333**:45–55 (2007). doi:10.1016/j.ijpharm.2006.09.048.
8. N. Y. K. Chew, and H. K. Chan. Use of solid corrugated particles to enhance powder aerosol performance. *Pharm. Res*. **18**:1570–1577 (2001). doi:10.1023/A:1013082531394.
9. N. Y. K. Chew, P. Tang, H. K. Chan, and J. A. Raper. How much particle surface corrugation is sufficient to improve aerosol performance of powders. *Pharm. Res*. **22**:148–152 (2005). doi:10.1007/s11095-004-9020-4.
10. H. Adi, D. Traini, H. K. Chan, and P. M. Young. The influence of drug morphology on aerosolisation efficiency of dry powder inhaler formulations. *J. Pharm. Sci*. **97**:2780–2788 (2008). doi:10.1002/jps.21195.
11. M. D. Louey, and P. J. Stewart. Particle interactions involved in aerosol dispersion of ternary interactive mixtures. *Pharm. Res*. **19**:1524–1531 (2002). doi:10.1023/A:1020464801786.
12. N. Islam, P. Stewart, I. Larson, and P. Hartley. Lactose surface modification by decantation: are drug-fine lactose ratios the key to better dispersion of salmeterol xinafoate from lactose-interactive mixtures. *Pharm. Res*. **21**:492–499 (2004). doi:10.1023/B:PHAM.0000019304.91412.18.
13. P. M. Young, D. Traini, H. K. Chan, H. Chiou, S. Edge, and T. Tee. The influence of mechanical processing dry powder inhaler carriers on drug aerosolisation performance. *J. Pharm. Sci*. **6**:1331–1341 (2007). doi:10.1002/jps.20933.
14. Y. Kawashima, T. Serigano, T. Hino, H. Yamamoto, and H. Takeuchi. Effect of surface morphology of carrier lactose on dry powder inhalation property of pranlukast hydrate. *Int. J. Pharm*. **172**:179–188 (1998). doi:10.1016/S0378-5173(98)00202-6.
15. F. Ferrari, D. Cocconi, R. Bettini, F. Giordano, P. Sant, M. J. Tobyn, R. Price, P. M. Young, C. Caramella, and P. Colombo. The surface roughness of lactose particles can be modulated by wet-smoothing using a high-shear mixer. *AAPS PharmSciTech*. **5**:1–6 (2004). doi:10.1208/pt050460.
16. D. El-Sabawi, S. Edge, R. Price, and P. Young. Continued investigation into the influence of loaded dose on the performance of dry powder inhalers: surface smoothing effects. *Drug Dev. Ind. Pharm*. **32**:1135–1138 (2006). doi:10.1080/03639040600712920.
17. J. N. Staniforth. Pre-formulation aspects of dry powder aerosols. *Proceedings of Respiratory Drug Delivery*. **1**:65–73 (1996).
18. P. M. Young, S. Edge, D. Traini, M. D. Jones, R. Price, D. El-Sabawi, C. Urry, and C. Smith. The influence of dose on the performance of dry powder inhalation systems. *Int. J. Pharm*. **296**:26–33 (2005). doi:10.1016/j.ijpharm.2005.02.004.
19. K. Iida, Y. Hayakawa, H. Okamoto, K. Danjo, and H. Leuenberger. Preparation of dry powder inhalation by surface treatment of lactose carrier particles. *Chem. Pharm. Bull*. **51**:1–5 (2003). doi:10.1248/cpb.51.1.
20. P. Begat, R. Price, H. Harris, D. A. V. Morton, and J. N. Staniforth. The influence of force control agents on the cohesive–adhesive balance in dry powder inhaler formulations. *Kona*. **23**:109–121 (2005).
21. P. Lucas, K. Anderson, U. J. Potter, and J. N. Staniforth. Enhancement of small particle size dry powder aerosol formulations using an ultra low density additive. *Pharm. Res*. **16**:1643–1647 (1999). doi:10.1023/A:1011981326827.
22. D. El-Sabawi, R. Price, S. Edge, and P. M. Young. Novel temperature controlled surface dissolution of excipient particles for carrier based dry powder inhaler formulations. *Drug Dev. Ind. Pharm*. **32**:243–251 (2006). doi:10.1080/03639040500466395.
23. M. D. Louey, S. Razia, and P. J. Stewart. Influence of physico-chemical carrier properties on the *in vitro* aerosol deposition from interactive mixtures. *Int. J. Pharm*. **252**:87–98 (2003). doi:10.1016/S0378-5173(02)00621-X.
24. P. M. Young, D. Roberts, H. Chiou, W. Rae, H. K. Chan, and D. Traini. Composite carriers improve the aerosolisation efficiency of drugs for respiratory delivery. *J. Aerosol Sci*. **39**:82–93 (2007). doi:10.1016/j.jaerosci.2007.10.003.
25. P. M. Young, D. Cocconi, P. Colombo, R. Bettini, R. Price, D. F. Steele, and M. J. Tobyn. Characterization of a surface modified dry powder inhalation carrier prepared by "particle smoothing". *J. Pharm. Pharmacol*. **54**:1339–1344 (2002). doi:10.1211/002235702760345400.
26. P. M. Young, R. Price, M. J. Tobyn, M. Buttrum, and F. Dey. Investigation into the effect of humidity on drug–drug interactions using the atomic force microscope. *J. Pharm. Sci*. **92**:815–822 (2003). doi:10.1002/jps.10250.
27. P. M. Young, M. J. Tobyn, R. Price, M. Buttrum, and F. Dey. The use of colloid probe microscopy to predict aerosolization performance in dry powder inhalers: AFM and *in vitro* correlation. *J. Pharm. Sci*. **95**:8100–1809 (2006).
28. J. H. Kirk, S. E. Dann, and C. G. Blatchford. Lactose: a definitive guide to polymorph determination. *Int. J. Pharm*. **334**:103–114 (2007). doi:10.1016/j.ijpharm.2006.10.026.
29. J. H. Bushill, W. B. Wright, C. H. F. Fuller, and A. V. Bell. Crystallisation of lactose with particular reference to its occurrence in milk powder. *J. Sci. Food Agric*. **16**:622–628 (1965). doi:10.1002/jsfa.2740161010.
30. R. Price, and P. M. Young. Visualization of the crystallization of lactose from the amorphous state. *J. Pharm. Sci*. **93**:155–164 (2004). doi:10.1002/jps.10513.
31. O. C. Chidavaenzi, G. Buckton, F. Koosha, and R. Pathak. The use of thermal techniques to assess the impact of feed concentration on the amorphous content and polymorphic forms present in spray dried lactose. *Int. J. Pharm*. **159**:67–74 (1997). doi:10.1016/S0378-5173(97)00272-X.
32. W.C. Hinds. *Aerosol Technology*. Willey, New York, 1999.
33. D. Traini, F. Thielmann, M. Acharya, K. Jarring, and P. M. Young. The influence of lactose pseudopolymorphism on salbutamol sulphate–lactose interactions in DPI formulations. *Drug Dev. Ind. Pharm*. **34**:992–1001.